STRESS DISTRIBUTION IN THE LIGAMENT ZONE OF PERFORATED CIRCULAR DISCS WITH SPECIAL REFERENCE TO THE STANDPIPE REGION OF THE PCPV FOR GAS-COOLED REACTORS

G. D. STEFANOU

Structural Analysis and Aseismic Research Laboratories,
The National Technical University, Athens, Greece

SUMMARY

The work presented herein relates to the distribution of long-term stresses within the ligaments of perforated circular concrete slabs, subjected to long-term radial loading and uniform elevated temperature. The perforations are reinforced with steel liners and arranged in a square central latice symmetrical about two orthogonal axes.

In order to assess the stress distribution around the perforated zone of a circular slab, a method of analysis was developed by the author, based on the "Equivalent Elastic Modulus" of the perforated zone, and the "Effective Modulus Method," utilizing experimental data obtained from tests performed on model specimens. The object of this paper is to extend the above method of analysis into the perforated region, and assess the long-term stresses in the ligaments.

The proposed method is accomplished by an application of the Finite Element Method for the elastic plane stress case. Comparisons of experimental results and theoretical predictions by the proposed method, and other analytical methods, are made for a series of perforated concrete slabs subjected to radial in-plane loading :10342 kN/m^2 (1500 psi), and uniform elevated temperature of 80°C. The investigation, though in general terms, could be applied to the perforated region of cylindrical pressure vessels for nuclear reactors.

H

1. INTRODUCTION

The distribution of stresses in the ligaments of perforated circular discs loaded in their plane has received a considerable amount of attention in recent years, and satisfactory elastic solutions have been obtained for particular cases. However, the distribution of long-term stresses has received little attention, and this is mainly due to lack of data.

A simplified method of analysis was developed by the writer and others (1) based on the Effective Modulus of the material, and on the Equivalent Elastic Modulus of the perforated zone of a circular disc having penetrations over its central area set on a rectangular square lattice and reinforced with steel liners.

It was possible by using the above method to assess the long-term stress distribution in the periphery of the perforated zone of the disc under both in-plane long-term radial loading and uniform elevated temperature. The method requires creep data for the calculation of the Effective Modulus of the material, and the assessment of the Equivalent Elastic Modulus of the perforated region. A full description of the method and the experimental work used is described in reference (1).

In this paper a method of analysis is described and is used to estimate the time-dependent stresses in the periphery and the ligaments of perforated discs. The method uses the Effective Modulus concept, and the Equivalent Elastic Modulus of the perforated zone, where allowance is made for the increasing creep with time and temperature, by reducing the elastic modulus throughout the area of the disc. The proposed method is accomplished by an application of the Finite Element displacement method for the two-dimensional plane-stress case, using triangular plate elements. A step-by-step analysis is adopted and solutions are obtained at desired intervals through a digital computer.

Experimental verification of the analysis for two different standpipe liners is reported and comparison with other solutions is made. The investigation could be applied to the perforated region of the end caps of cylindrical prestressed concrete pressure vessels (p.c.p.v) for nuclear reactors.

2. METHODS OF ANALYSIS - BASIC THEORY

The time-dependent analysis of stresses in perforated circular discs by the Finite Element displacement method, taking account of creep, is in general considerably more complex than elastic. When structures are operating at ambient temperatures, conventional elastic theory, using a reduced elastic modulus to allow for creep, may be employed confidently in many cases to calculate the stresses. The same approach, however, cannot be used, when thermal gradients exist, because considerable redistribution of stress in space and time then results, even when applied loads and temperatures do not vary with time. Creep data for the material must be obtained experimentally and the computations may have to be repeated at a number of time intervals, allowing for changes of external loading, temperature distributions, and material properties, which may be time-dependent.

2.1 The Effective Modulus Technique

The method of analysis described in this section is capable of predicting the redistribution of stresses which occur in heated concrete structures. The proposed method used the Effective Modulus concept where allowance is made for the increasing creep with time and temperature by selectively reducing the elastic modulus throughout the structure. Equations (1) and (2) define

$$E' = \frac{1}{E^{-1}+c} \qquad \ldots\ldots \qquad (1)$$

$$E' = \frac{1}{E^{-1}+c\phi(T)} \qquad \ldots\ldots \qquad (2)$$

the Effective Modulus E', which varies in time and space when temperature is not uniform. In expressions (1) and (2) above, $\phi(T)c$ represents the specific creep at the time considered, since $\sigma\phi(T)c$ corresponds to the creep component of the total strain under the sustained stress σ, and E is the elastic modulus of the material. This method of analysis which recognises the influence of time and temperature on the creep of concrete, by modifying the true elastic modulus, is simpler to use and becomes simply an analysis for a non-homogeneous elastic problem, for each time that is considered. The Effective Modulus is derived from experimental creep data, obtained under constant stress and temperature conditions.

2.2 The Finite Element Method As Applied To The Linear And Time-Dependent Problem

To incorporate the time-dependent creep effects in the analysis, the modulus of elasticity of the material is replaced by an equivalent Effective Modulus E', given in terms of the elastic modulus of the concrete and its specific creep, or its specific thermal creep strain, equations (1) and (2). An initial elastic solution is then carried out based on the two-dimensional Finite Element formulation using triangular plate elements. Descriptions of the method are available in numerous papers and a text book by O.C. Zienkiewicz (2), but as reference will be made to it frequently in this paper, the essentials of the Finite Element displacement method as applied to linear elastic problems are described briefly here.

The displacements $\{f\}$ of a typical element e, are defined in terms of its nodal displacements $\{\delta\}^e$ thus

$$\{f\} = [N]\{\delta\}^e \qquad \ldots\ldots \qquad (3)$$

where the matrix $[N]$ is a function of the nodal coordinates, and is known as the "shape function matrix." It is essential that the shape function matrix be defined in such a manner that continuity of displacements is preserved between the elements.

The element strains $\{e\}$ usually defined by derivatives of the element displacements $\{f\}$ can be determined in terms of nodal displacements as

$$\{\varepsilon\} = [B]\{\delta\}^e \qquad \ldots\ldots \qquad (4)$$

where $[B]$ is the coordinate transformation matrix.

From the element strains we calculate the element stresses $\{\sigma\}$ which are given in terms of the elasticity matrix $[D]$ by the equation:

$$\{\sigma\} = [D]\left(\{e\} - \{e_0\}\right) + \{\sigma_0\} \qquad \ldots\ldots \qquad (5)$$

in which $\{e_0\}$ is a set of independently developed "initial strains" and $\{\sigma_0\}$ is a system of "initial stresses."

If the externally applied loads $\{p\}$ corresponds with the element displacements $\{f\}$ then for a small change of nodal displacements $d\{f\}$ the variation of the potential energy $d(P)^e$ for an element is given as:

$$d(P)^e = \int \left(-\{p\}^T d\{f\} + \{\sigma\}^T d\{\varepsilon\}\right) dxdydz \qquad \ldots\ldots \qquad (6)$$

the integration taken over the volume of the element.

From equations (3) and (4), we note that

$$d\{f\} = [N]\,d\{\delta\}^e$$

$$d\{\varepsilon\} = [N]\,d\{\delta\}^e$$

and substituting these together with (5) in equation (6) we obtain

$$d(P)^e = \Big[\int (-\{p\}^T[N] + \{\sigma_o\}^T[B] - \{\varepsilon_o\}^T[D][B])\,dxdydz$$
$$+\{\delta^e\}^T\int [B]^T[D][B]\,dxdydz\Big]\,d\{\delta\}^e$$
$$= d\{\delta\}^{eT}\Big[\{F\}^e + [K]^e\{\delta\}^{eT}\Big] \qquad \ldots\ldots \qquad (7)$$

in which

$$\{F\}^e = +\int(-[N]^T\{p\} + [B]^T\{\sigma_o\} - [B][D]\{\varepsilon_o\})\,dxdydz$$

and

$$[K]^e = \int [B]^T\,[D]\,[B]\,dxdydz$$

where $\{F\}^e$ is the generalised element forces vector and $[K]^e$ the element stiffness matrix. The element forces and its stiffness matrix can be readily evaluated as all the quantities are known. For a solution giving the best approximation to equilibrium, the potential energy of the structure must be a minimum

$$\frac{d\,(P)}{d\,\{\delta\}} = 0$$

where $\{\delta\}$ are the structure displacements.

The above relation leads to a set of structural equations for displacements of the form

$$[K]\{\delta\} + \{F\} = 0 \qquad \ldots\ldots \qquad (8)$$

where $[K]_{rs} = \sum [K_{rs}]^e$ and,

$$\{F_r\} = \sum \{F_r\}^e$$

the summation taken over all elements.

By solving the system of equations (8), we obtain the unknown nodal displacements from which by use of equations (4) and (5), the element stresses can be evaluated.

After obtaining the initial elastic state of stress, the Effective Modulus E' of equation (1) or (2), is introduced in the elasticity matrix $[D]$ of equation (5), to give matrix $[D']$ which for isotropic materials and for the plane stress case it reduces to:

H

$$[D'] = \frac{E'}{(1-v^2)} \begin{bmatrix} 1 & v & 0 \\ v & 1 & 0 \\ 0 & 0 & \frac{1-v}{2} \end{bmatrix}$$

The elastic solution described in previous paragraphs is carried out again and may be repeated at any time interval when the stresses are required. Thermal and shrinkage effects may be dealt with readily if the thermal properties, and shrinkage strains of the discs material are known. They are introduced appropriately in the analysis by the thermal [Dt] and shrinkage [Ds] strain matrices respectively:

where $$[Dt] = a.dT \begin{Bmatrix} 1 \\ 1 \\ 0 \end{Bmatrix}, \text{ and } \quad Ds = \phi(T)\,ds \begin{Bmatrix} 1 \\ 1 \\ 0 \end{Bmatrix}$$

where a, is the coefficient of linear thermal expansion, dT and ds are increments of temperature and shrinkage strain and $\phi(T)$ a known temperature function.

2.3 The Computer Programme

Two approaches are mainly used to solve different structural problems in engineering by the Finite Element displacement method. The problem is to solve the large system of equilibrium equations for the unknown displacements. The first approach is usually referred to as the direct method using Gaussian elimination to invert the structure stiffness matrix [K]. The second approach is the iterative method and uses the Gauss-Seidel iteration technique for the solution of the equations. Currently, the most commonly used programmes are based on these two techniques, descriptions of which can be found in published papers by Zienkiewcz (2) & Argyris (3).

In general, when calculating the time-dependent stresses in heated structures, the material properties, the external loads and dimensions all vary in space and time. In this general case, the structure stiffness matrix [K] has to be recalculated and its inverse formed at each time-step. If the material properties and the geometry do not vary with time, and only the loads are changing, then only the right hand side of equation (8) has to be recalculated at each time interval, and the stiffness matrix [K] and its inverse have to be calculated only once.

In the present development the direct method using Gaussian elimination was used for the solution of the equations. The advantages gained in solving the equations by matrix inversion, are the reduction of computational effort and the greater accuracy in determining the unknown displacements. The greatest disadvantage of this method is the storage required by the stiffness matrix. It was partly overcome by making use of the band width and the "shifted matrix."

The programme is coded in FORTRAN language and was originally written for the CDC6600 computer of the University of London. It incorporates the general Finite Element procedure for two-dimensional elastic, thermoelastic, creep and shrinkage analyses. Two-dimensional triangular plate elements were used to represent the structural system.

The programme performs three major tasks; a) generates the equilibrium equations of the structural system; b) solves these equations for the nodal point displacements by direct elimination, and uses a step-by-step procedure which permits accounting for the time-dependent material properties; and c) calculates the stresses and strains relative to the element.

2.4 The Equivalent Elastic Modulus Concept

The term "Equivalent Elastic Modulus", Ee, is used to define the apparent modulus of elasticity of the perforated region of the disc. The perforated zone can be considered to be replaced by an equivalent homogeneous material with notional material properties Fig. 1 (a),(b). It can be defined directly by either loading the perforated disc and measuring or calculating the strains across one of its diameters. For the case of the fully perforated disc the equivalent elastic modulus can be calculated by Sheffield's proposal briefly described in Appendix 1. With the equivalent elastic modulus of the perforated region known, we may now proceed in the calculation of stress distribution around the periphery. An initial elastic solution at time T1 will give the stress distribution in the periphery of the perforated zone

$$P1 = \frac{e_{e1}}{1/_{Ee1}} \quad \ldots\ldots \quad (9)$$

under sustained load and temperature the material of the disc will creep and the new stress distribution at time T2 will be given by:

$$P2 = \frac{e_{e1} + e_{c2}}{1/_{Ee2 + c_2}} \quad \ldots\ldots \quad (10)$$

In the equations(9) and (10)above, e_{ei} is the elastic strain at time t_i, Eei is the equivalent elastic modulus of the zone at time t_i, e_{ci} is the creep strain and $c = \frac{e_{ci}}{\sigma_i}$ is the specific creep of the disc's material at time t_i.
The creep data must be obtained experimentally. The application of the method is described in Appendix 2.

3. APPLICATION OF THE PROPOSED METHOD OF ANALYSIS

The developed method of analysis was used to predict the variation of stress and strains in the periphery of the perforated zone, and in the ligaments, for two series of perforated concrete discs, subjected to in-plane radial loading of 1500 psi., and uniform elevated temperature of 80^{o}C.

The thickness of the reinforcing liners for the two series of test were 1/4" and 3/16" respectively. Numerical solutions for the discs under the temperature and loading regimes shown in Fig. (2), were obtained. The dimensions of the discs were taken as: External diameter of disc $d_e = 36"$. Diameter of the central perforated region $d_p = 13\ 3/4"$. Radial load $p = 1500$ psi. For the concrete the elastic constants were: Coefficient of linear thermal expansion of concrete $a_c = 12.8\text{x}10^{-6}$ strain units per centrigrade degree, Young's modulus of concrete $E = 5.0\text{x}10^{6}$ lb/in2, Poisson's ratio of concrete $v_c = 0.18$, and for the steel these were: $E_s = 30.0\text{x}10^{6}$ lb/m2, $v_s = 0.30$.

The temperature function $\emptyset(T)$ was approximated by a second order polynomial in (T) of the form

$$\emptyset(T)=k_o + k_1(T)+k_2(T)^2$$

and the values of the constants k_o, k_2 determined from experimental results of reference (4), giving $k_o= -7.64$, $k_1 = 1.09$ and $k_2 = 0.006$. The creep function $\emptyset(T)c$ was approximated by a logarithmic curve in two parts again from reference (4), data.

$$\left.\begin{array}{l}(\emptyset(T)c)_t=1.51\text{x}10^{-9}\log(1+t) \text{ for } 0 \leq t \leq 50 \text{ days and} \\ (\emptyset(T)c)_t=(3.62\text{x}\log(1+t)-3.58)\text{x}10^{-9} \text{ for } t > 50 \text{ days}\end{array}\right\}$$

The variation of stress and strains with time were calculated for several time intervals and plotted against a time basis corresponding to the test programme. See figures (3) to (9) inclusive.

4. APPLICATION OF THE DISC SOLUTION IN CONCRETE PRESSURE VESSELS

The geometry of the discs tested and the loading and temperature regimes applied were chosen as being fairly typical of those in the top end closure of a cylindrical prestressed concrete pressure vessel, a sketch of which is shown in Fig. (10). In these vessels, the central region is penetrated by a large number of standpipes used for loading

the reactor. The loading and end conditions to which these caps are subjected are well known and can be summarised thus:-
In-plane radial compression, transverse loading, peripheral restraining moments from the walls, varying temperature gradients across the slab, and difference in average temperatures between the slab and the wall.

In a general analysis of a whole pressure vessel, all the above loadings can be included and the resulting stresses assessed. However, from the present development only in-plane radial compression and uniform elevated temperature have been considered, and for these conditions the problem of the disc may have an application for the assessment of the effects of creep on the behaviour of the vessel.

5. DISCUSSION OF RESULTS OF THE DISC-CONCLUSSIONS.

The analytical time-dependent solution of perforated circular concrete discs subjected to radial pressure and uniform elevated temperature has been presented. It has been shown that the Effective Modulus concept coupled with the equivalent elastic modulus of the perforated zone introduced by the writer in reference (1), to calculate the load distribution around the periphery of the zone, can be extended into the perforated region, and assess the long-term stresses in the ligaments.

A study of figure (3), shows that in both cases, there is a decay of stress with time in the periphery of the perforated central region of the disc and appears to be due to the difference in the rate of creep between the perforated zone and the concrete in the annulus. On application of heat, a rapid increase in the stress is disclosed and this is mainly due to the restrained thermal expansion. It is worth mentioning that during the tests, the perforated zone was at a higher temperature than that of the surrounding concrete in the annulus. The reduction in stress for the two series of discs tested is relatively small, and therefore, should not cause any serious damage to a real structure.

The radial and tangential stresses in the concrete within the ligaments were computed by the proposed method and were compared with those obtained by the rate of creep method (5).
As expected, a decay of stresses with time was predicted by both methods, see figures (4), (5), (6) and (7).

Radial and tangential concrete strains were predicted by the described method and were compared with those obtained experimentally.

It is seen from figures (8) and (9) that the diametral strains were under-estimated and the tangential strains were over-estimated.

APPENDIX 1

THE EFFECTIVE MODULUS AND THE EQUIVALENT ELASTIC MODULUS OF PERFORATED REGION FOR CALCULATING THE STRESS DISTRIBUTION

An analysis has been carried out based on the Effective Modulus method and the Equivalent Elastic Modulus of perforated zone to calculate the load distribution around the periphery of the penetrations of a 36" diameter concrete disc (Fig. 1), loaded in its plane by a radial load of 1500 psi., and a uniform elevated temperature of 80°C.

The results obtained from the analysis are presented in analytical and graphical form (Figs., (3) to (9)(inclusive), at seven different phases of the test programme. The data used in the analysis were obtained from curves drawn from experimental observations during the test programme.

The equivalent elastic modulus and the creep and shrinkage data required for the perforated zone of the 36" specimen were obtained from curves drawn from experimental observations during the test programme. The equivalent elastic modulus and the creep and shrinkage data required from a 16 3/4" diameter perforated specimen. The values so obtained were checked by Sheffield's proposal and appropriately used in the analysis for the various times considered.

The stresses were checked at seven different phases of the test programme: 1) at time T1 when the load was applied to obtain the elastic stresses; 2) at time T2 before heating commenced to obtain stress due to creep strains at ambient temperature; 3) at time T2 after heating was applied to calculate the thermoelastic stresses due to restrained thermal expansion; 4) at time T3 before heating was removed to obtain the stresses and to forecast the effects of thermal creep on the disc; 5) at time T3 after heating was removed; 6) at time T4 before unloading and 7) at time T4 after unloading.

The notation and sign convention used throughout the analysis are shown in Fig. 11 (a),(b), and Fig. 12 (a),(b). The subscripts, e, c, s, and t, refer to elastic, creep shrinkage and temperature respectively.

The following relations were used in the calculations:

1) at time T1 equation (9) is used.

2) at time T2 before application of heat, equation (10) is used.

3) at time T3 after application of heat.

a) including thermoelastic effects.

$$p'_2 = \frac{e_{c1} + de_{t2} + e_{c2}}{1/Ee2 + {}_{c2}} \qquad \ldots\ldots \quad (11)$$

b) excluding thermoelastic effects.

$$p'_2 = \frac{e_{e1} + e_{c2}}{1/Ee2 + {}_{c2}} \qquad \ldots\ldots \quad (12)$$

4) at time T3 before heat was removed.

a) thermoelastic effect included

$$p_3 = \frac{e_{e1} + de_{t2} + e_{c3}}{1/Ee3 + {}_{c3}} \qquad \ldots\ldots \quad (13)$$

b) thermoelastic effect excluded

$$p'_3 = \frac{e_{e1} + e_{c3}}{1/Ee3 + {}_{c3}} \qquad \ldots\ldots \quad (14)$$

5) at time T3 after heat was removed

$$p'_3 = \frac{e_{e1} + de_{t2} - de_{t3} + e_{c3}}{1/Ee3 + {}_{c3}} \qquad \ldots\ldots \quad (15)$$

6) at time T4 before load was removed

a) thermoelastic effect included

$$p_4 = \frac{e_{e1} + de_{t2} - de_{t3} + e_{c4}}{1/Ee3 + {}_{c4}} \qquad \ldots\ldots \quad (16)$$

b) thermoelastic effect excluded

$$p^*_4 = \frac{e_{e1} + e_{c4}}{1/Ee3 + {}_{c4}} \qquad \ldots\ldots \quad (17)$$

7) at time T4 after load was removed

$$p'_4 = \frac{e_{e1} + de_{t2} - de_{t3} + e_{c4} - e_{c4}}{1/Ee3 + {}_{c4}} \qquad \ldots\ldots \quad (18)$$

The stress distribution obtained from the analysis in the periphery of the perforated zone is shown in figure (3).

APPENDIX 2

ANALYTICAL CALCULATION OF THE EQUIVALENT ELASTIC MODULUS OF PERFORATED ZONE OF THE DISC.

1) Perforations without reinforcing liners.

It is assumed that the plate figure (13), has a uniform external pressure p and contains n circular holes with a uniform applied pressure p_i around the i-th hole. The shear forces are taken as zero on all the bounding curves.

For a single circular plate without apertures the stress function U due to uniform external pressure has to form $(C+B_r 2)$, where $\underline{r}$ is measured from the centre of the plate. Similarly, a single hole with uniform internal pressure in an infinite plate, has a stress function (D + A log r), where r is now taken from the centre of the hole. A stress function of the following form is considered.

$$U(\underline{r}) = \frac{Q}{2} r.r + \sum_{i=1}^{n} A_i \log/\underline{r} - \underline{r}i/ \quad \ldots\ldots \quad (19)$$

For free inner boundaries of the holes, having the same radii and equal interval pressures, it may be proved that the stress function of equation (19) would assume the following form:

$$U(r) = - \frac{-p}{1-n\mu} \frac{\underline{r}.\underline{r}}{2} - a^2 \sum_{i-1}^{n} \log/\underline{r} - \underline{r}_i / \quad \ldots\ldots \quad (20)$$

where $\mu_j = \frac{a_j^2}{a_o^2}$ (j,=1, ...n), $\underline{r} = (r,\theta)$, as the radius of the plate and a_o the radius of the i-th hole.

For the case of p = p the stress function assumes the simple form

$$U(r) = - \frac{pr^2}{2} \quad \ldots\ldots \quad (21)$$

Differenciating equation (20) we obtain

$$(\sigma_r + \sigma_\theta) = - \frac{2p}{1-n\mu} \quad \ldots\ldots \quad (22)$$

At the outer boundary

$$\sigma_r = - p \quad \ldots\ldots \quad (23)$$

We define Effective Young's Modulus Ee and Effective Poisson's Ratio v_e to be the value of a uniform disc which is of the same size as the perforated plate, and which suffers the same displacements as the perforated plate. When subjected to the same system of stresses no simple value of Ee and v_e will make this possible for all applied stresses, so we shall require the boundary displacements to be the same when both plates are subjected to the same uniform external pressure p.

The stress function of the uniform plate is then given by equation (21), and if $(\sigma_r)_e$ and $(\sigma_\theta)_e$ are the stresses for this plate

$$(\sigma_r)_e + (\sigma_\theta)_e = -2p \qquad \ldots\ldots \quad (24)$$

if E and r refer to the material of the perforated plate, we have

$$\frac{\sigma_\theta - v\ \sigma_r}{E} = \frac{(\sigma_\theta)_e - v_e\,(\sigma_r)_e}{Ee} \qquad \ldots\ldots \quad (25)$$

Substituting the values of σ_θ σ_r, $(\sigma_\theta)_e$ and $(\sigma_r)_e$ obtained from equations (22), (23) and (24), we have:

$$\frac{Ee}{E} = \frac{1-v_e}{\frac{2}{1-n\mu} - (1+v)} = \frac{1-v_e}{\frac{1+n\mu}{1-n\mu} - v} \qquad \ldots\ldots \quad (26)$$

Now

$$n = \frac{na^2}{d^2} = \frac{n(a^2\pi)}{\pi d^2} = \frac{nA_h}{Ap} = \Omega$$

where nA_h = total area of holes

Ap = total area of plate

Thus equation (8) may be written

$$\frac{Ee}{E} = \frac{1-v_e}{\left(\frac{1+\Omega}{1-\Omega}\right) - v} \qquad \ldots\ldots \quad (27)$$

If we assume $v = v_e$ we have a simple formula with which an average Effective Young's Modulus can be calculated for any value of v of the plate. The above formula has been studied for free edge inner boundaries and for the particular case of v = 0.3 in an infinite lattice of interval holes.

2) **Perforations with reinforcing liner's**

The ratio Ee/Ec is given by the following equation:

$$\frac{Ee}{Ec} = \frac{1-v_c}{\frac{1+\Omega(1-2G)}{1-\Omega} - v_c} \qquad \ldots\ldots \quad (28)$$

where

$$G = \frac{(1-v_e)\ Es}{\left(\frac{2A_h - As}{As} - v_s\right)\ Ec} \qquad \ldots\ldots \quad (29)$$

REFERENCES

(1) STEFANOU G.D., YU C.W.,GILL S. An experimental investigation into the behaviour of perforated end slabs for concrete pressure vessels under temperature and external load. Internation Conference on model techniques for prestressed concrete pressure vessels. The British Nuclear Energy Society, London, July, 1969.

(2) ZIENKIEWICZ O.C. The finite element method in structural continuum mechanics. McGraw-Hill, London, 1967.

(3) ARGYRIS J.G., KELSEY S. Energy theorems and structural analysis.

(4) HANNAT D.J. Strain behaviour of concrete upto 95°C under compressive stresses. Proc. Conf., on P.C.P.V., 1967, Inst., Civil Engineers, London, pp.177-191.

(5) STEFANOU .D. A theoretical and experimental investigation into the perforated zones of nuclear reactor pressure vessels. London University, Ph.D. Thesis, 1970.

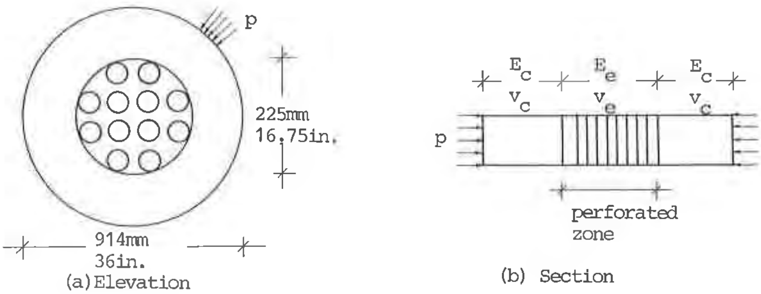

Fig. 1. Perforated disc

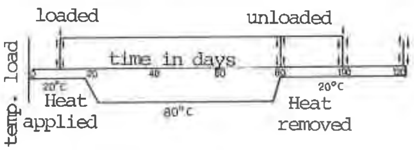

Fig.2. Temperature and loading regime

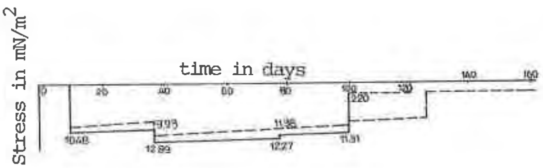

Fig.3. Stress distribution in the periphery of the perforated zone
(Standpipe thickness 1.59mm----------)
(Standpipe thickness 6.35mm ————)

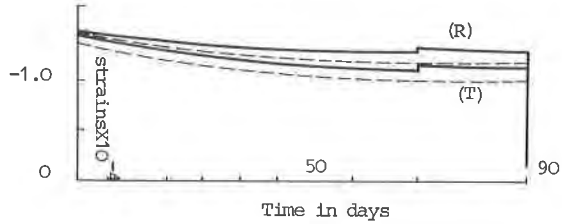

Fig.4. Series 2: Tangential (T), and radial stresses (R)
Effective Mondulus method (E.M.)----------
Rate of Creep method (R.C.) ————

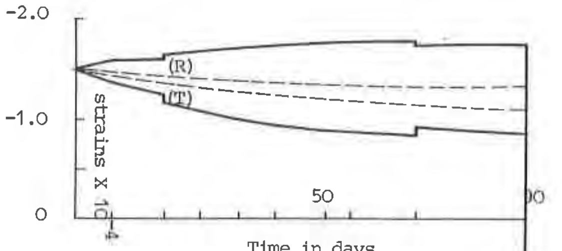

Fig.5 Series 2: Tangential (T), and radial (R) stresses
(E.M.)----------- , (R.C.)————

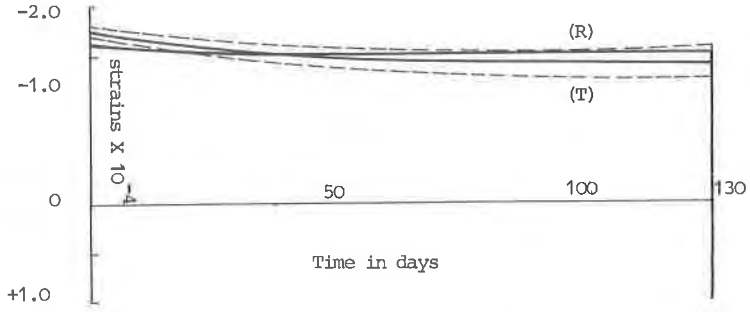

Fig. 6 Series 1: Tangential (T), and radial (R) stresses
(E.M.)------------, (R.C.) ————

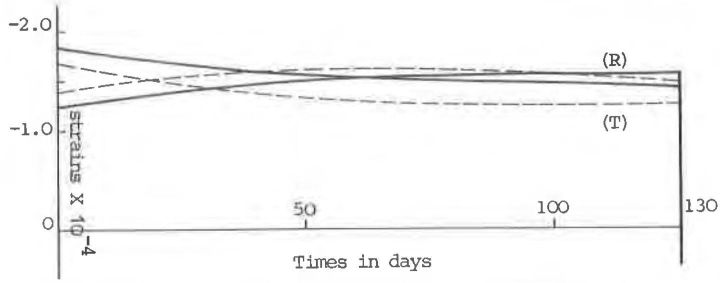

Fig. 7. Series 1: Tangential (T) and radial (R) stresses
(E.M)———— (R.C.)————

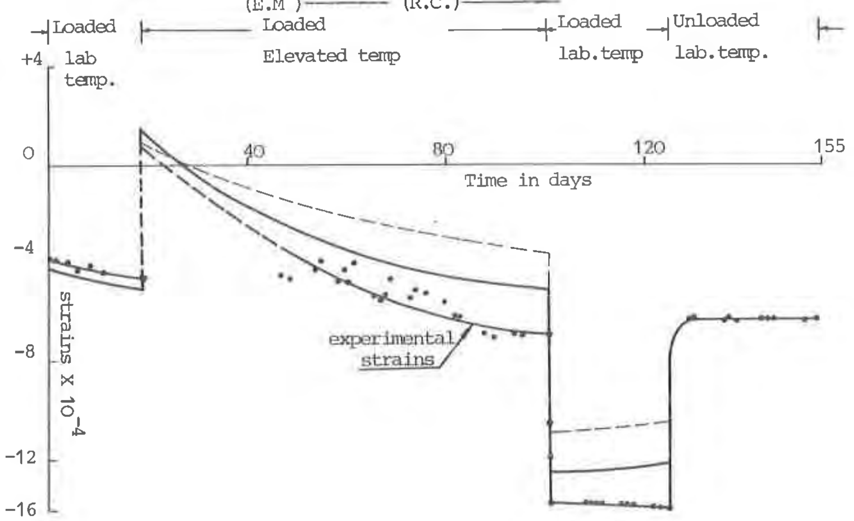

Fig. 8. Series 1: Diametral gross strains,perforated zone
(E.M.)-----, (R.C.)————

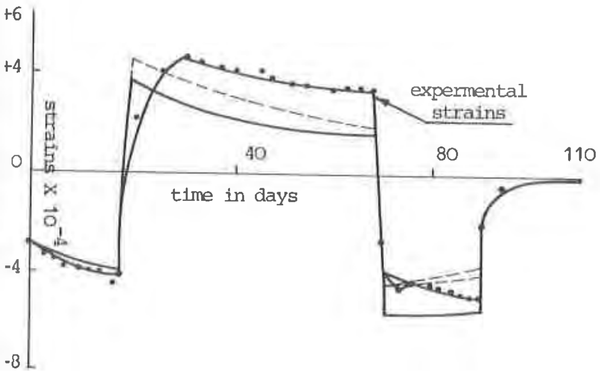

Fig. 9. Series 2: Radial gross strains,perforated zone
(E.M)-------, (R.C.)————

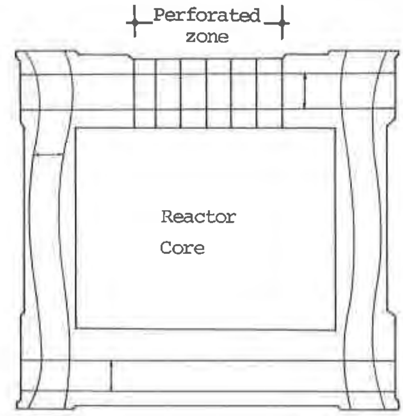

Fig. 10.Section of a cylindrical
P.C.P.Vessel

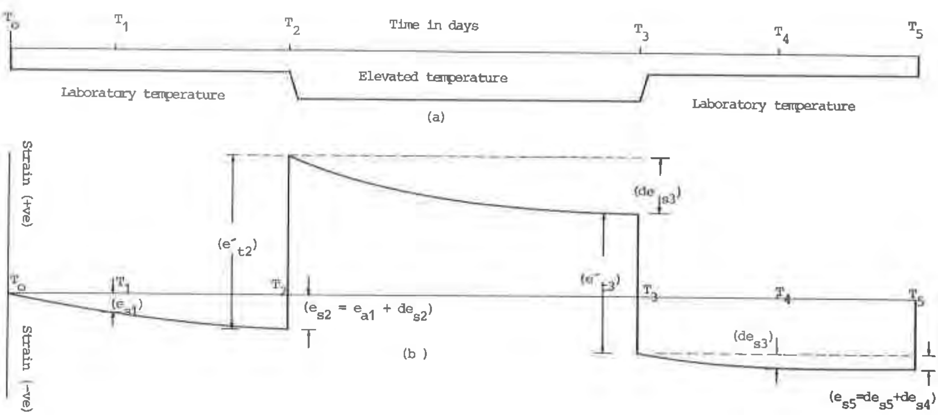

FIG.11. Typical shrinkage time curve for unloaded specimens.

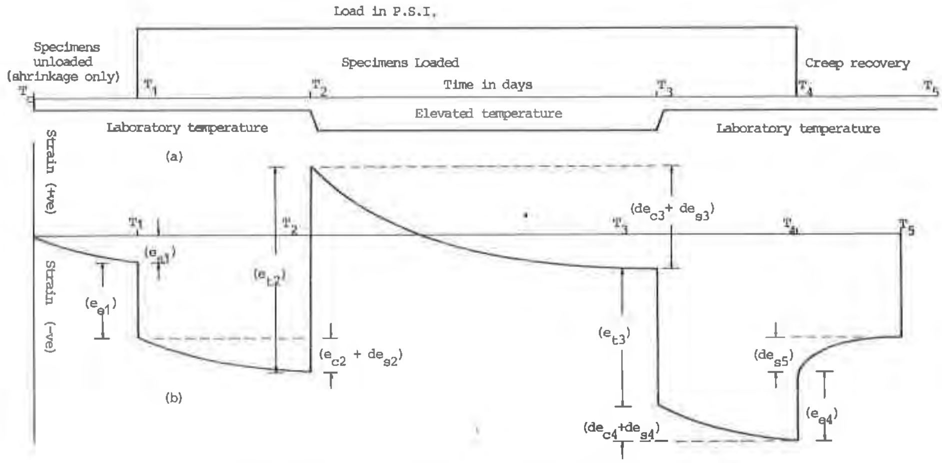

FIG.12 Typical Strain-Time curve for loaded specimens.

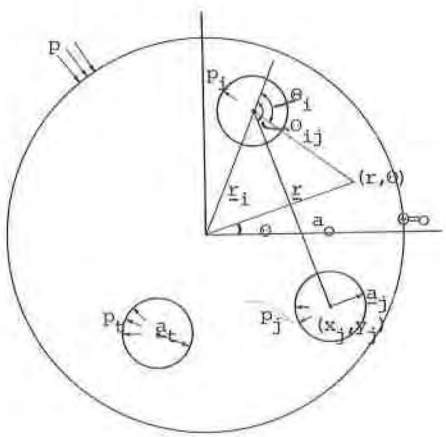

Fig. 13